A Current Decoupling Parallel Control Strategy of Single-Phase Inverter With Voltage and Current Dual Closed-Loop Feedback

Shungang Xu, Jinping Wang, and Jianping Xu, *Member, IEEE*

***Abstract*—The output characteristics of a single-phase inverter with voltage and current dual closed-loop feedback control are analyzed, and the equivalent circuit model of a parallel single-phase inverter system is introduced. By taking both resistance and inductance components of the equivalent output impedance into consideration, a current decoupling control strategy of the parallel inverter system is then proposed. Furthermore, by constructing a three-phase balanced current according to the output current of the single-phase inverter, an active and reactive current decomposition method is presented to decompose the output current of the single-phase inverter into active and reactive currents according to the instantaneous reactive power theory. The block diagram of the active and reactive current decomposition method is given, and current decomposition simulation results are shown to verify the analysis results. The prototype is developed, and the control of two parallel-connected 2-kVA inverters is realized. The experimental results show its feasibility and effectiveness.**

***Index Terms*—Circulating current, instantaneous reactive power theory, parallel inverter.**

I. Introduction

PARALLEL operation of inverters is an effective way to increase the power capacity and the reliability of inverter systems. One of the key concerns of the parallel inverter system is the distribution of load current among parallel-connected inverters. Only when the parallel-connected inverters have the same amplitude, frequency, and phase can the load current be evenly distributed among parallel-connected inverters. Due to differences of circuit parameters and line impedance mismatches among parallel-connected inverters, it is difficult to keep the output voltages of all the parallel-connected inverters have the same amplitude, frequency, and phase. Due to small output impedance of the inverter, any slight difference of output voltages among parallel-connected inverters may lead to great circulating current in the parallel inverter system, which will affect the efficiency and lead to overload or damage of the inverters [1]–[8].

Manuscript received March 16, 2011; revised May 13, 2011; accepted June 18, 2011. Date of publication July 14, 2011; date of current version November 22, 2012. This work was supported in part by the National Natural Science Foundation of China under Grant 50677056 and in part by the Fundamental Research Funds for the Central Universities under Grant SWJTU09ZT13. This paper was presented in part at the Second IEEE Energy Conversion Congress and Exposition, Atlanta, GA, September 12–16, 2010.

The authors are with the School of Electrical Engineering, Southwest Jiaotong University, Chengdu 610031, China (e-mail: shungang_xu@163.com; waupter919@163.com; jpxu-swjtu@163.com).

Digital Object Identifier 10.1109/TIE.2011.2161660

Control techniques for the parallel inverter system can be classified into two main groups according to control wire interconnections [9]. The first one is based on active load sharing techniques derived from control schemes of parallel-connected dc–dc converters, such as centralized [10], [11], master–slave [12], [13], average load sharing [14], [15], and circular chain control [16], [17]. Although these control methods achieve good output voltage regulation and current sharing, intercommunication lines among inverters are required, which will reduce system reliability and expandability [18].

The second one is mainly based on power droop theory, which benefits with no requirement of physical control wire interconnections [19]–[32]. It realizes the control of parallel inverter systems by adjusting the frequency and amplitude of output voltage as a function of active and reactive powers delivered by the inverter. The power droop method achieves higher reliability and flexibility as only local power measurements are used. Nevertheless, the conventional power droop control usually assumes that the output impedance of the inverter is purely inductive due to the inductor filter, and neglects the influence of its resistance. However, the closed-loop output impedance of the inverter heavily depended on the control parameters and frequency, and the line impedance is predominantly resistive, particularly for low-voltage cabling. Additionally, the computation of active and reactive powers according to conventional power theory is based on average voltage and average current, which suffers from drawbacks such as slow transient response, tradeoff among power-sharing accuracy, the deviation of frequencies and output voltages, unbalance of harmonic current sharing, and high dependence on output impedance of the inverter [18].

In this paper, with regard to single-phase inverters with voltage and current dual closed-loop feedback control, the output characteristics of the inverter are analyzed, and the equivalent circuit model of the parallel inverter system is given. By taking both resistance and inductance components of the equivalent output impedance into consideration, a current decoupling control strategy of the parallel inverter system is then proposed.

Furthermore, by constructing a three-phase balanced current according to the output current of the single-phase inverter, an active and reactive current decomposition method is presented to decompose the output current of the single-phase inverter into active and reactive currents according to the instantaneous reactive power theory, which features benefits of good transient response and simplified control algorithm realization.

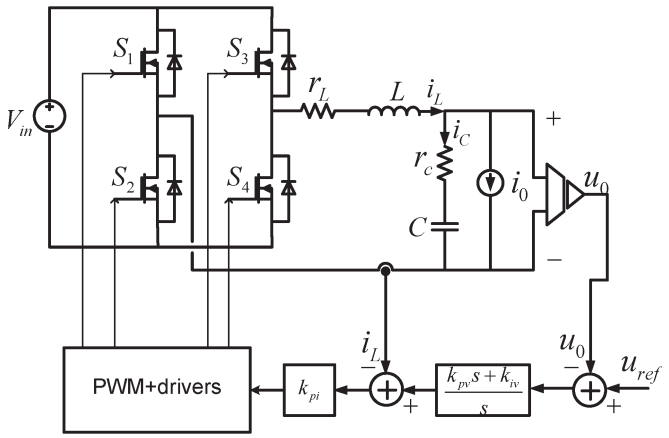

Fig. 1. Single-phase inverter with dual closed-loop feedback control.

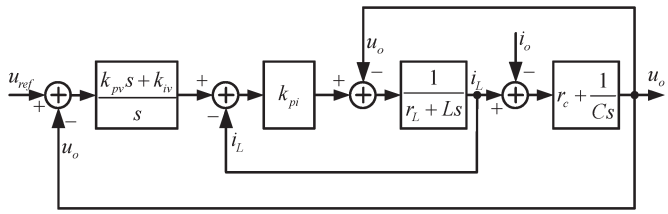

Fig. 2. Block diagram of the output voltage controller of single-phase inverter.

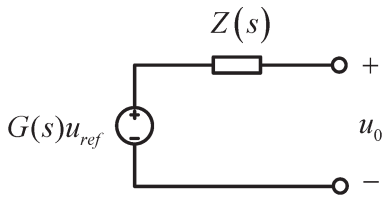

Fig. 3. Equivalent circuit of single-phase inverter.

The block diagram of the active and reactive current decomposition method is given, and the simulation results well verify the analysis results. Furthermore, the prototype is developed, and the control of two parallel-connected 2-kVA inverters is realized. The experimental results show its feasibility and effectiveness.

This paper is organized as follows. In Section II, the equivalent output impedance of the single-phase inverter is analyzed. The equivalent circuit model and the controller design of the parallel single-phase inverter system are presented in Section III. An active and reactive current decomposition method based on instantaneous reactive power theory is proposed, and the simulation results of the proposed method and the conventional method are presented in Section IV. The experimental results are given in Section V to verify the analysis results, and the conclusion is given in Section VI.

II. Output Characteristics of Single-Phase Inverter

Capacitor voltage and inductor current dual closed-loop feedback control, as shown in Fig. 1, is usually adopted for the control of single-phase inverters [33]–[36], where the proportional–integral control in the outer loop is utilized to realize output voltage control, with $k_{\rm pv}$ and $k_{\rm iv}$ as the corresponding proportional and integral coefficients, respectively, while, in the inner loop, proportional control is used to improve the transient response of the inverter, with $k_{\rm pi}$ as the proportional coefficient.

In Fig. 1, r_L and r_c are parasitic parameters of the circuit, with r_L representing the effect of equivalent series resistance (ESR) of the output filter inductor, the on resistance of the switches, the dead-time effects of full-bridge switches, and the resistance of the connection line and r_c representing the ESR of the output filter capacitor. According to state-space averaging approach [37], the full bridge can be equivalent to a proportional amplifier with unit gain. Then, the block diagram of the output voltage controller of the single-phase inverter can be given as shown in Fig. 2. The closed-loop output voltage can be expressed as

$$u_o = G(s)u_{\rm ref} - Z(s)i_o \tag{1}$$

where $G(s)$ is the gain coefficient and $Z(s)$ is the equivalent output impedance of the inverter, respectively. See (2) and (3), shown at the bottom of the page.

From (2) and (3), we can know that $G(s)$ and $Z(s)$ are closely related to filter parameters L and C, closed-loop control parameters $k_{\rm pv}, k_{\rm iv},$ and $k_{\rm pi}$, and parasitic parameters of the circuit r_L and r_c.

Thus, the single-phase inverter with voltage and current dual closed-loop feedback control can be regarded as the series of an ideal voltage source and the equivalent output impedance of the inverter, with its equivalent circuit as shown in Fig. 3.

From (3), we can know that the equivalent output impedance is usually of complex impedance characteristic and heavily depends on the parameters of the output filter, the control parameters of the feedback control loop, and the parasitic parameters of the circuit.

For the analysis of the equivalent output impedance of the single-phase inverter, the following parameters are used: $L = 500\ \mu$H, $C = 10\ \mu$F, $k_{\rm pv} = 5$, $k_{\rm iv} = 100$, $k_{\rm pi} = 1$, and the parasitic parameters r_L and r_c are 0, 0.2, 0.4, and 0.6 Ω,

$$G(s) = \frac{k_{\rm pv}k_{\rm pi}r_cCs^2 + (k_{\rm pi}k_{\rm iv}r_cC + k_{\rm pv}k_{\rm pi})s + k_{\rm pi}k_{\rm iv}}{LCs^3 + (r_LC + k_{\rm pi}C + k_{\rm pv}k_{\rm pi}r_cC + r_cC)s^2 + (1 + k_{\rm pv}k_{\rm pi} + k_{\rm iv}k_{\rm pi}r_cC)s + k_{\rm pi}k_{\rm iv}} \tag{2}$$

$$Z(s) = \frac{r_cLCs^3 + (L + k_{\rm pi}r_cC + r_Lr_cC)s^2 + (k_{\rm pi} + r_L)s}{LCs^3 + (r_LC + k_{\rm pi}C + k_{\rm pv}k_{\rm pi}r_cC + r_cC)s^2 + (1 + k_{\rm pv}k_{\rm pi} + k_{\rm iv}k_{\rm pi}r_cC)s + k_{\rm pi}k_{\rm iv}} \tag{3}$$

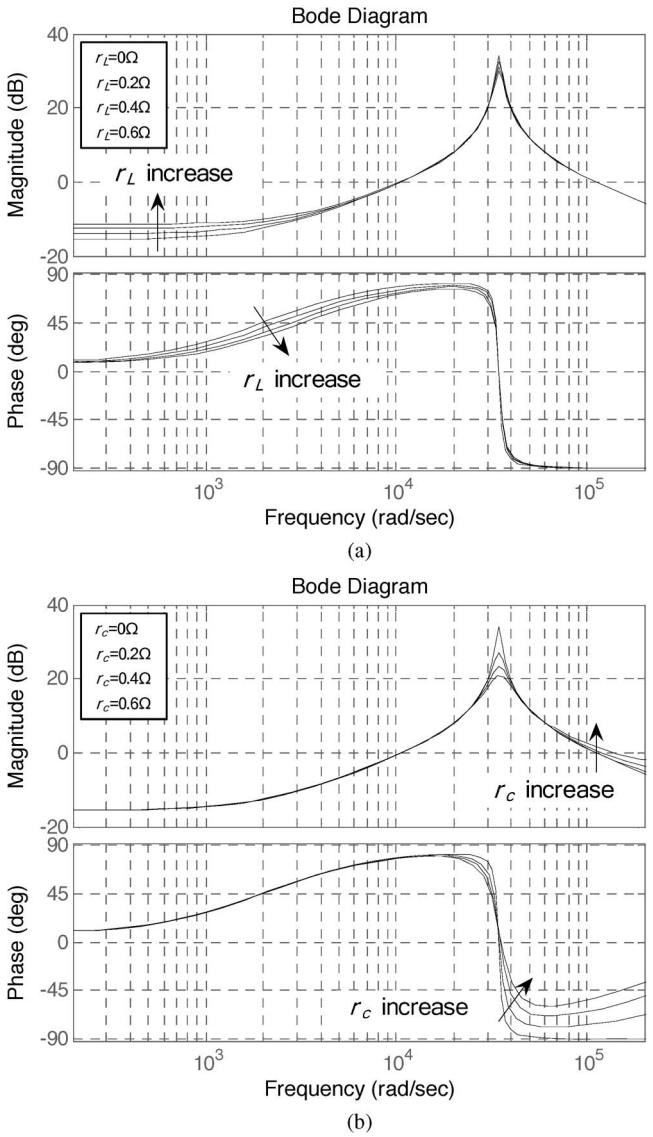

Fig. 4. Bode diagram of the output impedance. (a) Output impedance with different r_L's. (b) Output impedance with different r_c's.

respectively. The corresponding Bode diagrams of the output impedance can be depicted as shown in Fig. 4.

From Fig. 4(a), we can know that parasitic parameter r_L has great influence on the output impedance at low frequency, with the output impedance increasing along with the increase of r_L. From Fig. 4(b), we can know that parasitic parameter r_c has great effect on the output impedance at high frequency.

In the parallel inverter system, the output impedance of each inverter has significant effect on the power flow and the design of the control circuit. From (3), it can be known that the equivalent output impedance tends to be resistive with the increase of the control parameters $k_{\rm pv}$ and $k_{\rm pi}$ and tends to be inductive with the decrease of the control parameter $k_{\rm iv}$. As the parameters affect not only the transient response of the inverter but also the current sharing performance of the parallel inverter system, the control parameter design of the dual closed-loop feedback single-phase inverter is important.

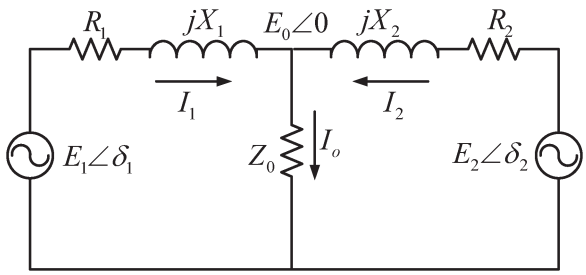

Fig. 5. Equivalent circuit model of single-phase parallel inverter.

III. Controller Design of Parallel Single-Phase Inverter

Due to the complex impedance characteristic of the equivalent output impedance, it can be regarded as the series of resistors and inductors. Therefore, the equivalent circuit model of the single-phase parallel inverter with voltage and current dual closed-loop feedback control can be given as shown in Fig. 5, where $E_1\angle\delta_1$ and $R_1 + jX_1$ are the output voltage and equivalent output impedance of inverter I, $E_2\angle\delta_2$ and $R_2 + jX_2$ are the output voltage and equivalent output impedance of inverter II, Z_0 is the load of the parallel inverter system, and $E_0\angle 0$ is the output voltage across the load.

From the equivalent circuit of the single-phase parallel inverter, the output current of each inverter can be given as

$$\begin{cases} I_1 = \frac{E_1(\cos\delta_1 + j\sin\delta_1) - E_0}{R_1 + jX_1} \\ I_2 = \frac{E_2(\cos\delta_2 + j\sin\delta_2) - E_0}{R_2 + jX_2}. \end{cases} \tag{4}$$

The circulating current of the parallel inverter system is defined as [38]

$$I_H = \frac{I_1 - I_2}{2}. \tag{5}$$

In the parallel inverter system, the power angles δ_1 and δ_2 are very small; thus, we can assume that $\cos\delta_1 = 1$, $\cos\delta_2 = 1$, $\sin\delta_1 = \delta_1$, and $\cos\delta_2 = \delta_2$. In order to decrease the difference among the inverters, the parameters of each inverter should be designed as the same, i.e., $R_1 = R_2 = R$ and $X_1 = X_2 = X$. Then, the active and reactive circulating currents can be derived as

$$\begin{cases} i_{\rm hp} = \frac{R\Delta E + XE\Delta\delta}{2(R^2 + X^2)} \\ i_{\rm hq} = \frac{RE\Delta\delta - X\Delta E}{2(R^2 + X^2)} \end{cases} \tag{6}$$

where $\Delta E = E_1 - E_2$ and $\Delta\delta = \delta_1 - \delta_2$. Therefore, the active and reactive circulating currents are related to both the amplitude and the phase difference of inverters in the parallel system.

In the parallel inverter system, the differences of the active and reactive output currents lead to the unbalance of load current among inverters. The relation between the active/reactive output current and output voltage amplitude/phase is defined by (6). Therefore, the block diagram of the decoupling control strategy can be given as shown in Fig. 6. Each inverter decouples the active and reactive components of the circulating current to regulate the amplitude and phase of the output voltage.

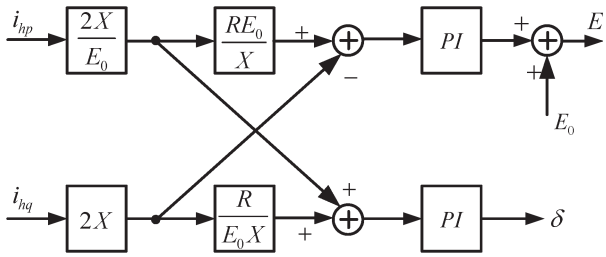

Fig. 6. Block diagram of decoupling control strategy.

From (6), we can also know that the performance of active and reactive current decomposition heavily affects the parallel operation performance.

IV. Output Current Decomposition and Simulation Analysis of Single-Phase Inverter

In the parallel inverter system, the decomposition of active and reactive currents may have great effect on load sharing performance of the system. However, conventional-power-theory-based computation of active and reactive powers is calculated from average voltage and average current, which suffers from drawbacks such as slow transient response, tradeoff among power-sharing accuracy, the deviation of frequencies and output voltages, unbalance of harmonic current sharing, and high dependence on the inverter output impedance [18]. To overcome these drawbacks, Akagi et al. proposed the instantaneous reactive power theory [39], which can decompose three-phase instantaneous current into active and reactive currents. This algorithm can calculate the instantaneous active and reactive currents without delay. However, the instantaneous reactive power theory is originally developed for three-phase power systems and cannot be directly applied to the calculation of active and reactive currents of single-phase inverters.

As the output voltage of the inverter is regularly sinusoidal wave, to calculate the active and reactive currents of the single-phase inverter by instantaneous reactive power theory, we can construct a three-phase balanced current by using the output current of the single-phase inverter with phase shift. Then, the constructed voltage and current can meet the conditions of the instantaneous reactive power theory and can be used to calculate the active and reactive components of the single-phase inverter.

A. Active and Reactive Output Current Decomposition of Single-Phase Inverter

The output voltage of the single-phase inverter can be expressed as

$$u_o = U_m \sin \omega t. \tag{7}$$

As the inverter may supply nonlinear loads, the output current may contain high-order harmonic components. Thus, the output current can be expressed as

$$\begin{aligned} i_o =& I_1 \sin(\omega t + \varphi) + \sum_{n=2}^{\infty} I_n \sin(n\omega t + \varphi_n) \\ =& I_1 \cos\varphi \sin\omega t + I_1 \sin\varphi \cos\omega t + \sum_{n=2}^{\infty} I_n \sin(n\omega t + \varphi_n) \\ =& i_p + i_q + i_h \end{aligned} \tag{8}$$

where I_1 and I_n are the amplitudes of the fundamental and the nth-order harmonic current and i_p, i_q, and i_h are the active, reactive, and harmonic currents, respectively. They can be rewritten as

$$i_p = I_1 \cos\varphi \sin\omega t = I_p \sin\omega t \tag{9}$$

$$i_q = I_1 \sin\varphi \cos\omega t = I_q \cos\omega t \tag{10}$$

$$i_h = \sum_{n=2}^{\infty} I_n \sin(n\omega t + \varphi_n). \tag{11}$$

We can regard the output current i_o of the single-phase inverter as a phase current i_{La} of a three-phase system

$$i_{La} = i_o = I_1 \sin(\omega t + \varphi) + \sum_{n\geq 2} i_{an}. \tag{12}$$

Then, by delaying the phase current i_{La} by $\pi/(3\omega)$ and inversing it, we get another phase current of the three-phase system as

$$\begin{aligned} i_{Lc} =& -I_1 \sin\left(\omega\left(t - \frac{\pi}{3\omega}\right) + \varphi\right) + \sum_{n\geq 2} i_{cn} \\ =& I_1 \sin\left(\omega t + \frac{2\pi}{3} + \varphi\right) + \sum_{n\geq 2} i_{cn}. \end{aligned} \tag{13}$$

We can further construct the last phase current of the three-phase system from i_{La} and i_{Lc} as

$$i_{Lb} = -i_{La} - i_{Lc} = I_1 \sin\left(\omega t - \frac{2\pi}{3} + \varphi\right) + \sum_{n\geq 2} i_{bn}. \tag{14}$$

i_{La}, i_{Lb}, and i_{Lc} constitute a balanced three-phase current, and i_{xn} (x is a, b, or c) is the nth-order harmonic component of the phase current. Then, according to the instantaneous reactive power theory [39]–[41], the transformation matrix is

$$C_{\alpha\beta} = \frac{2}{3}\begin{bmatrix} 1 & -\frac{1}{2} & -\frac{1}{2} \\ 0 & \frac{\sqrt{3}}{2} & -\frac{\sqrt{3}}{2} \end{bmatrix} \tag{15}$$

$$C_{pq} = \begin{bmatrix} \sin\omega t & -\cos\omega t \\ -\cos\omega t & -\sin\omega t \end{bmatrix} \tag{16}$$

where $\sin\omega t$ and $\cos\omega t$ are of the same frequency and phase as the fundamental harmonics of the single-phase inverter output voltage. Then, d–q transformation can be used to transform the balanced three-phase currents i_{La}, i_{Lb}, and i_{Lc} into the α–β-axis, and the instantaneous current components on the α–β-axis can be expressed as follows:

$$\begin{bmatrix} i_\alpha \\ i_\beta \end{bmatrix} = C_{\alpha\beta}\begin{bmatrix} i_{La} \\ i_{Lb} \\ i_{Lc} \end{bmatrix} = \begin{bmatrix} I_1 \sin(\omega t + \varphi) + \sum_{n=2}^{\infty} i_{\alpha h_n} \\ -I_1 \cos(\omega t + \varphi) + \sum_{n=2}^{\infty} i_{\beta h_n} \end{bmatrix} \tag{17}$$

where $i_{\alpha h_n}$ and $i_{\beta h_n}$ are the nth-order harmonic current components. Then, the active and reactive currents can be expressed

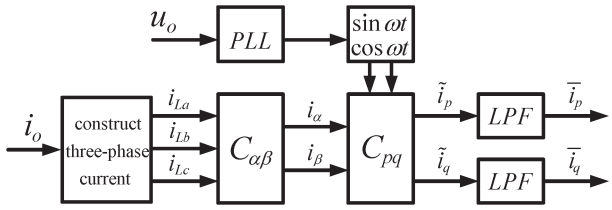

Fig. 7. Block diagram of the proposed active and reactive current decomposition method.

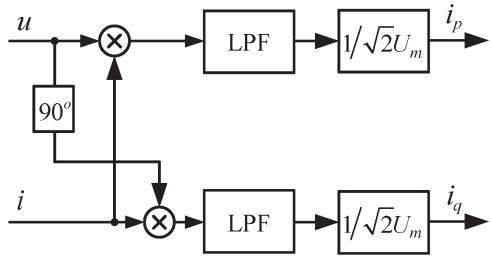

Fig. 8. Block diagram of conventional active and reactive current decomposition method.

as follows:

$$\begin{bmatrix}\tilde{i}_p\\ \tilde{i}_q\end{bmatrix} = C_{pq}\begin{bmatrix}i_\alpha\\ i_\beta\end{bmatrix} = \begin{bmatrix}I_1\cos\varphi + \sum\tilde{i}_{ph_n}\\ -I_1\sin\varphi + \sum\tilde{i}_{qh_n}\end{bmatrix} = \begin{bmatrix}I_p + \sum\tilde{i}_{ph_n}\\ -I_q + \sum\tilde{i}_{qh_n}\end{bmatrix}. \tag{18}$$

In (18), $\tilde{i}_{ph_n}$ and $\tilde{i}_{qh_n}$ are the nth-order harmonic current components. After an appropriate low-pass filter (LPF) is used to filter all the high-order harmonic components $\sum\tilde{i}_{ph_n}$ and $\sum\tilde{i}_{qh_n}$, then $\bar{i}_p$ and $\bar{i}_q$ are equal to the amplitudes of the active and reactive currents of the single-phase inverter, respectively, as shown in the following equation:

$$\begin{bmatrix}\bar{i}_p\\ \bar{i}_q\end{bmatrix} = \begin{bmatrix}I_p\\ -I_q\end{bmatrix}. \tag{19}$$

The block diagram of the proposed three active and reactive current decomposition can be shown as Fig. 7. $\sin\omega t$ and $\cos\omega t$ are produced by the digital phase-locked loop (PLL) circuit [42], [43], which can dynamically track the output voltage frequency and phase of the single-phase inverter. The LPFs are used to filter the high-frequency harmonic current components of the active and reactive output currents.

B. Simulation Analysis of the Active and Reactive Output Current Decomposition

Fig. 9 shows the simulation results of the active and reactive currents calculated by using the proposed method and the conventional method, where $i_{p-\mathrm{pm}}$ and $i_{q-\mathrm{pm}}$ are the active and reactive currents calculated by the proposed method, with the cutoff frequency of second-order LPF as 50 Hz, $i_{p-\mathrm{cm}}$ and $i_{q-\mathrm{cm}}$ are the active and reactive currents calculated by the conventional method, as shown in Fig. 8, with the cutoff frequency of second-order LPF as 10 Hz, and U_m is the amplitude of the voltage u.

The simulation results, as shown in Fig. 9, are obtained under three different load conditions, with the current step

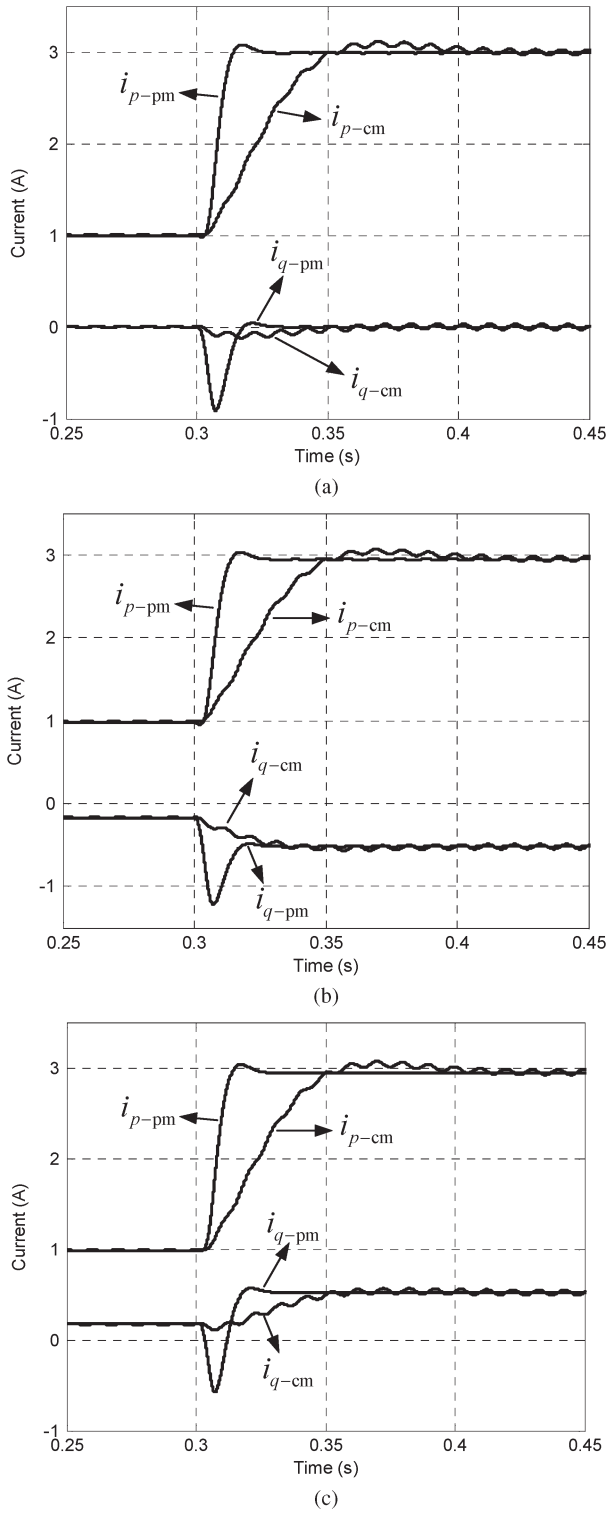

Fig. 9. Simulation results of current decomposition by the proposed and conventional active and reactive current decomposition methods. (a) Under pure resistive load condition. (b) Under resistive–inductive load condition. (c) Under resistive–capacitive load condition.

increased from 1 to 3 A at 0.3 s. Fig. 9(a) shows the case under pure resistive load condition, where the voltage and current are in phase with each other. Similarly, Fig. 9(b) and (c) shows the cases under resistive–inductive load condition and resistive–capacitive load condition where the current lags and leads the voltage 10°, respectively.

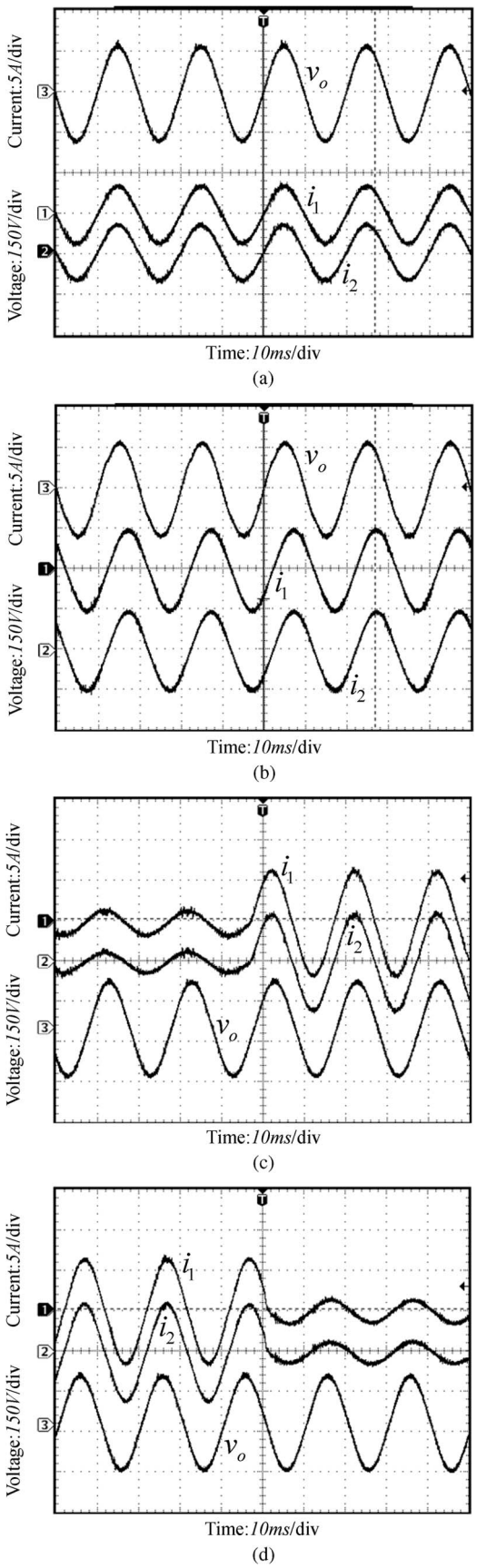

Fig. 10. Experiment waveforms of parallel inverter. (a) Steady-state waveform under resistive load. (b) Steady-state waveform under resistive–inductive load. (c) Transient waveforms under step-up load variation. (d) Transient waveforms under step-down load variation.

As shown in Fig. 9, the steady active and reactive currents of the proposed composition method are not influenced by the fluctuation of the voltage and current while the conventional method should choose lower cutoff-frequency LPF to smooth the fluctuation of active and reactive currents, which means longer response time in transient conditions. Simultaneously, the proposed method can make the active and reactive currents recover to steady state within 20 ms under step current variation, while the conventional method needs longer time.

V. Experiment Results

Based on the aforementioned discussion, an experimental prototype of parallel operation of two 2-kVA single-phase inverters is built, with an output filter inductance of 500 μH, a filter capacitance of 10 μF, a dc input voltage of 200 Vdc, and an ac output voltage of 110 Vac with a frequency of 50 Hz.

The closed-loop control of the inverter, the decoupling strategy, the active and reactive current decomposition based on the instantaneous reactive power theory, the phase lock of the output voltage, and the sinusoidal pulse width modulation (SPWM) signal generator are all realized by a digital signal processor.

Experimental results of the two parallel-connected inverters are shown in Fig. 10. Fig. 10(a) and (b) shows the steady performance of the parallel inverter system, from which it can be known that, under purely resistive load, the output currents of these two inverters are 2.82 and 2.79 A, respectively, and, under resistive–inductive load, the output currents are 3.49 and 3.57 A, respectively. Thus, good load sharing can be achieved in steady state.

The dynamic performances of the two parallel-connected inverters under step load variation are also shown in Fig. 10(c) and (d), from which it can be known that the proposed control method has good dynamic response performance.

VI. Conclusion

In the single-phase parallel inverter system with dual closed-loop feedback control, the circulating current is closely related not only to the amplitude and phase of the inverter reference signal but also to the control parameters of the closed-loop feedback. Based on the analysis of the equivalent circuit model of the single-phase parallel inverter system, a current decoupling control strategy of the parallel inverter system has been proposed, which decomposes the output current into active and reactive components according to the instantaneous reactive power theory. The active and reactive currents are decoupled to regulate the amplitude and phase of the output voltage, respectively. By using the instantaneous reactive power theory to decompose the active and reactive currents of the single-phase inverter, the proposed decoupling control strategy obtains good transient response performance and has the features of simplified algorithm, fast calculation speed, and easy digital processing.

References

[1] X. Sun, L. K. Wong, Y. S. Lee, and D. H. Xu, "Design and analysis of an optimal controller for parallel multi-inverter systems," *IEEE Trans. Circuits Syst. II, Exp. Briefs*, vol. 53, no. 1, pp. 56–61, Jan. 2006.

[2] F. S. Pai, J. M. Lin, and S. J. Huang, "Design of an inverter array for distributed generations with flexible capacity operations," *IEEE Trans. Ind. Electron.*, vol. 57, no. 12, pp. 3927–3934, Dec. 2010.
[3] Y. Q. Pei, G. B. Jiang, and X. Yang, "Auto-master–slave control technique of parallel inverters in distributed AC power systems and UPS," in *Proc. Power Electron. Spec. Conf.*, Aachen, Germany, 2004, pp. 2050–2053.
[4] K. Siri, T. F. Wu, and C. Q. Lee, "Current distribution control schemes for parallel connected converter modules part I: Master–slave control," *IEEE Trans. Aerosp. Electron. Syst.*, vol. 28, no. 3, pp. 829–840, Jul. 1992.
[5] P. C. Loh, M. J. Newman, and D. N. Zmood, "A comparative analysis of multi-loop voltage regulation strategies for single and three-phase UPS systems," *IEEE Trans. Power Electron.*, vol. 18, no. 5, pp. 1176–1185, Sep. 2003.
[6] C. Cecati, F. Ciancetta, and P. Siano, "A multilevel inverter for photovoltaic systems with fuzzy logic control," *IEEE Trans. Ind. Electron.*, vol. 57, no. 12, pp. 4115–4125, Dec. 2010.
[7] L. Xiao, W. B. Hu, and Y. G. Yan, "Summary of the control techniques of paralleled inverters," in *Proc. APSC*, Nanjing, China, 2000.
[8] A. Tuladhar, H. Jin, T. Unger, and K. Mauch, "Control of parallel inverters in distributed AC power systems with consideration of line impedance effect," *IEEE Trans. Ind. Appl.*, vol. 36, no. 1, pp. 131–137, Jan./Feb. 2000.
[9] J. M. Guerrero, L. G. de Vicuña, and J. Uceda, "Uninterruptible power supply systems provide protection," *IEEE Ind. Electron. Mag.*, vol. 1, no. 1, pp. 28–38, 2007.
[10] A. P. Martins, A. S. Carvalho, and A. S. Araújo, "Design and implementation of a current controller for the parallel operation of standard UPSs," in *Proc. IEEE IECON*, 1995, pp. 584–589.
[11] T. Iwade, S. Komiyama, and Y. Tanimura, "A novel small-scale UPS using a parallel redundant operation system," in *Proc. IEICE/IEEE INTELEC*, 2003, pp. 480–483.
[12] W.-C. Lee, T.-K. Lee, S.-H. Lee, K.-H. Kim, D.-S. Hyun, and I.-Y. Suh, "A master and slave control strategy for parallel operation of three phase UPS systems with different ratings," in *Proc. IEEE APEC*, 2004, pp. 456–462.
[13] Y. J. Cheng and E. K. K. Sng, "A novel communication strategy for decentralized control of paralleled multi-inverter systems," *IEEE Trans. Power Electron.*, vol. 21, no. 1, pp. 148–156, Jan. 2006.
[14] X. Sun, Y.-S. Lee, and D. Xu, "Modeling, analysis, and implementation of parallel multi-inverter system with instantaneous average-current-sharing scheme," *IEEE Trans. Power Electron.*, vol. 18, no. 3, pp. 844–856, May 2003.
[15] Y. Xing, L. Huang, S. Sun, and Y. Yan, "Novel control for redundant parallel UPSs with instantaneous current sharing," in *Proc. IEEE PCC Conf.*, Osaka, Japan, 2002, pp. 959–963.
[16] T. F. Wu, Y.-K. Chen, and Y.-H. Huang, "3C strategy for inverters in parallel operation achieving an equal current distribution," *IEEE Trans. Ind. Electron.*, vol. 47, no. 2, pp. 273–281, Apr. 2000.
[17] S. J. Chiang, C. H. Lin, and C. Y. Yen, "Current limitation control technique for parallel operation of UPS inverters," in *Proc. IEEE Power Electron. Spec. Conf.*, 2004, pp. 1922–1926.
[18] J. M. Guerrero, L. Hang, and J. Uceda, "Control of distributed uninterruptible power supply systems," *IEEE Trans. Ind. Electron.*, vol. 55, no. 8, pp. 2845–2859, Aug. 2008.
[19] C. J. Zhang, G. T. Chen, Z. N. Guo, and W. Y. Wu, "An alternating-master–salve parallel control research for single phase paralleled inverters based on CAN bus," in *Proc. IPEMC*, Shanghai, China, 2006, pp. 1–5.
[20] J. M. Guerrero, L. G. de Vicuña, J. Matas, M. Castilla, and J. Miret, "A wireless controller to enhance dynamic performance of parallel inverters in distributed generation systems," *IEEE Trans. Power Electron.*, vol. 19, no. 5, pp. 1205–1213, Sep. 2004.
[21] J. M. Guerrero, L. G. de Vicuña, J. Matas, M. Castilla, and J. Miret, "Output impedance design of parallel-connected UPS inverters with wireless load-sharing control," *IEEE Trans. Ind. Electron.*, vol. 52, no. 4, pp. 1126–1135, Aug. 2005.
[22] J. M. Guerrero, J. Matas, L. G. de Vicuña, M. Castilla, and J. Miret, "Wireless-control strategy for parallel operation of distributed generation inverters," *IEEE Trans. Ind. Electron.*, vol. 53, no. 5, pp. 1461–1470, Oct. 2006.
[23] J. M. Guerrero, N. Berbel, J. Matas, J. L. Sosa, and L. G. de Vicuña, "Control of line-interactive UPS connected in parallel forming a microgrid," in *Proc. IEEE ISIE*, 2007, pp. 2667–2672.
[24] J. M. Guerrero, L. G. de Vicuña, and J. Uceda, "Uninterruptible power supply systems provide protection," *IEEE Ind. Electron. Mag.*, vol. 1, no. 1, pp. 28–38, 2007.
[25] J. M. Guerrero, J. C. Vásquez, J. Matas, M. Castilla, and L. G. de Vicuña, "Control strategy for flexible microgrid based on parallel line-interactive UPS systems," *IEEE Trans. Ind. Electron.*, vol. 56, no. 3, pp. 726–736, Mar. 2009.
[26] M. C. Chandorkar, D. M. Divan, Y. Hu, and B. Banerjee, "Novel architectures and control of distributed UPS systems," in *Proc. APEC*, Orlando, FL, 1994, pp. 683–689.
[27] J. M. Guerrero, L. G. de Vicuña, J. Matas, and J. Miret, "A wireless controller to enhance dynamic performance of parallel inverters in distributed generation systems," *IEEE Trans. Power Electron.*, vol. 19, no. 5, pp. 1205–1213, Sep. 2004.
[28] Y. B. Byun, T. G. Koo, and K. Y. Joe, "Parallel operation of three-phase UPS inverters by wireless load sharing control," in *Proc. INTELEC*, Phoenix, AZ, 2000, pp. 526–532.
[29] K.-S. Low and R. Cao, "Model predictive control of parallel-connected inverter for uninterruptible power supplies," *IEEE Trans. Ind. Electron.*, vol. 55, no. 8, pp. 2884–2893, Aug. 2008.
[30] M. Pascual, G. Garcerá, E. Figueres, and F. González-Espín, "Robust model-following control of parallel UPS single-phase inverters," *IEEE Trans. Ind. Electron.*, vol. 55, no. 8, pp. 2870–2883, Aug. 2008.
[31] J. M. Guerrero, J. C. Vasquez, J. Matas, L. G. de Vicuña, and M. Castilla, "Hierarchical control of droop-controlled AC and DC microgrids—A general approach toward standardization," *IEEE Trans. Ind. Electron.*, vol. 58, no. 1, pp. 158–172, Jan. 2011.
[32] X. F. Wang, J. M. Guerrero, Z. Chen, and F. Blaabjerg, "Distributed energy resources in grid interactive AC microgrids," in *Proc. PEDG*, Heifei, China, 2010, pp. 806–812.
[33] X. Sun, Y. S. Lee, and D. H. Xu, "Modeling, analysis, and implementation of parallel multi-inverter systems with instantaneous average-current-sharing scheme," *IEEE Trans. Power Electron.*, vol. 18, no. 3, pp. 844–856, May 2003.
[34] M. Castilla, J. Miret, J. Matas, L. G. de Vicuna, and J. M. Guerrero, "Linear current control scheme with series resonant harmonic compensator for single-phase grid-connected photovoltaic inverters," *IEEE Trans. Ind. Electron.*, vol. 55, no. 7, pp. 2724–2733, Jul. 2008.
[35] J. C. Vásquez, J. M. Guerrero, E. Gregorio, P. Rodríguez, R. Teodorescu, and F. Blaabjerg, "Adaptive droop control applied to distributed generation inverters connected to the grid," in *Proc. IEEE ISIE*, 2008, pp. 2420–2425.
[36] M. Liserre, R. Teodorescu, and F. Blaabjerg, "Multiple harmonics control for three-phase grid converter systems with the use of PI-RES current controller in a rotating frame," *IEEE Trans. Power Electron.*, vol. 21, no. 3, pp. 836–841, May 2006.
[37] J. P. Xu and C. Q. Lee, "A unified averaging technique for the modeling of quasi-resonant converters," *IEEE Trans. Power Electron.*, vol. 13, no. 3, pp. 556–563, May 1998.
[38] Z. H. Ye, D. Boroyevich, and J. Y. Choi, "Control of circulating current in two parallel three-phase boost rectifiers," *IEEE Trans. Power Electron.*, vol. 17, no. 5, pp. 609–615, Sep. 2002.
[39] H. Akagi, Y. Kanazawa, and A. Nabae, "Instantaneous reactive power compensators comprising switching devices without energy storage components," *IEEE Trans. Ind. Appl.*, vol. IA-20, no. 3, pp. 625–630, May 1984.
[40] F. Z. Peng, G. W. Ott, Jr., and D. J. Adams, "Harmonic and reactive power compensation based on the generalized instantaneous reactive power theory for three-phase four-wire systems," *IEEE Trans. Power Electron.*, vol. 13, no. 6, pp. 1174–1181, Nov. 1998.
[41] V. Soares, P. Verdelho, and G. D. Marques, "An instantaneous active and reactive current component method for active filters," *IEEE Trans. Power Electron.*, vol. 15, no. 4, pp. 660–669, Jul. 2000.
[42] L. G. B. Rolim, D. R. da Costa, and M. Aredes, "Analysis and software implementation of a robust synchronizing PLL circuit based on the pq theory," *IEEE Trans. Ind. Electron.*, vol. 53, no. 6, pp. 1919–1926, Dec. 2006.
[43] J. W. Choi, Y. K. Kim, and H. G. Kim, "Digital PLL control for single phase photovoltaic system," *Proc. Inst. Elect. Eng.—Elect. Power Appl.*, vol. 153, no. 1, pp. 40–46, Jan. 2006.

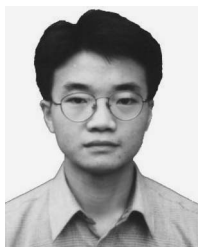

Shungang Xu was born in Chongqing, China, in 1975. He received the M.S. degree from the University of Electronic Science and Technology of China, Chengdu, China, in 2006. He is currently working toward the Ph.D. degree in the School of Electrical Engineering, Southwest Jiaotong University, Chengdu.

His research interests include DSP-based digital control technique, photovoltaic generation, high-power converters, and energy storage systems for electronic vehicles.

Jinping Wang was born in Hunan, China, in 1984. He received the B.S. degree in electronic and information engineering from Southwest Jiaotong University, Chengdu, China, in 2007, where he is currently working toward the Ph.D. degree in the School of Electrical Engineering.

His research interests include control technique and modulation method of switching-mode power supplies and modeling and simulation of switching dc–dc converters.

Jianping Xu (M'09) received the B.S. and Ph.D. degrees in electronic engineering from the University of Electronic Science and Technology of China, Chengdu, China, in 1984 and 1989, respectively.

Since 1989, he has been with the School of Electrical Engineering, Southwest Jiaotong University, Chengdu, where he has been a Professor since 1995. From November 1991 to February 1993, he was a Visiting Research Fellow with the Department of Electrical Engineering, University of Federal Defense, Munich, Germany. From February 1993 to July 1994, he was a Visiting Scholar with the Department of Electrical Engineering and Computer Science, University of Illinois, Chicago. His research interests include modeling, analysis, and control of power electronic systems.